

RSC Advances

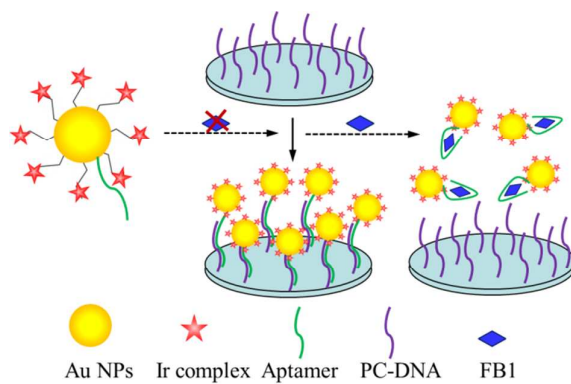


This is an *Accepted Manuscript*, which has been through the Royal Society of Chemistry peer review process and has been accepted for publication.

Accepted Manuscripts are published online shortly after acceptance, before technical editing, formatting and proof reading. Using this free service, authors can make their results available to the community, in citable form, before we publish the edited article. This *Accepted Manuscript* will be replaced by the edited, formatted and paginated article as soon as this is available.

You can find more information about *Accepted Manuscripts* in the [Information for Authors](#).

Please note that technical editing may introduce minor changes to the text and/or graphics, which may alter content. The journal's standard [Terms & Conditions](#) and the [Ethical guidelines](#) still apply. In no event shall the Royal Society of Chemistry be held responsible for any errors or omissions in this *Accepted Manuscript* or any consequences arising from the use of any information it contains.



TOC Figure

A simple gold nanoparticles-Ir complex driven electrochemiluminescence aptasensors was fabricated for the sensitive detection of Fumonisin B1.

Au NPs driven electrochemiluminescence aptasensors for sensitive detection of Fumonisin B1

Cite this: DOI: 10.1039/x0xx00000x

Yuan Zhao, Yaodong Luo, Tongtong Li, Qijun Song*

Received 00th January 2014,
Accepted 00th January 2014

DOI: 10.1039/x0xx00000x

www.rsc.org/

In this study, a simple gold nanoparticles (Au NPs) driven electrochemiluminescence (ECL) aptasensors was fabricated for the sensitive detection of Fumonisin B1 (FB1), taking advantages of the weak background noise and good ECL efficiency of the ionic iridium (Ir) complex, the high affinity and specificity of aptamers for targets, as well as the large specific surface and excellent conductivity of Au NPs. Different amounts of Ir complex were loaded on the surface of Au NPs through mercaptoethylamine. Au NPs-Ir complex served as a nanoprobe was applied in the development of ECL-aptasensor, and a limit of detection (LOD) as low as 0.27 ng/mL was achieved for the FB1. The proposed method not only has high sensitivity, but also showed good accuracy and stability. The principle proposed in this paper could be widely applicable in the development of nanomaterials-driven ECL-aptasensors for other mycotoxin detection.

Introduction

Fumonisin is a group of mycotoxins primarily produced by *Fusarium moniliforme*, and are one of the most common fungi colonizing corn throughout the world.¹ FB1 is the most investigated mycotoxin and can cause harmful diseases including cancer on human and animal.^{2, 3} Researchers are striving for sensitive FB1 detection for many years, but mainly focus on enzyme-linked immunosorbent assay (ELISA),² lateral-flow strip,^{4, 5} traditional instrumental analysis⁶ and other assays.⁷⁻⁹ ELISA, due to the complicated and multi-step operations and the false-positive results, limited its application in FB1 determination.¹⁰ The instrumental methods not only required expensive instruments, but often also depended on the complex purification and manipulation steps.⁶ Even though low LOD for FB1 detection were reported with the use of fluorescence methods, however, these methods were often interfered by the strong background emission from the biology matrix and the quenching effects by oxygen, humidity and foreign species.⁷⁻⁹ Hence it was still imperative to develop a simple, low cost and accurate method to achieve high sensitive detection of the FB1.

ECL-aptasensors, as an alternative method to the fluorescence method, had gained considerable research interests in recent years, attributing to the fact that the ECL methods had a number of intrinsic advantages, including (1) the good ECL efficiency, low background noise and high sensitivity of ECL systems;¹¹⁻¹⁴ (2) the high affinity and specificity of aptamers for targets,¹⁵⁻¹⁷ as well as the advantages of aptamers against antibodies such as low cost, thermal and chemical stability with long shelf life, structure reversible ability and easy functionalized with ECL labels.^{12, 18} They were successfully applied for the detection of DNA,¹¹ thrombin^{13, 19, 20} and toxins.¹² Aptamers for FB1 had been successfully screened and showed specific and high affinity to FB1 with a dissociation

constant of 100 ± 30 nM.¹⁵ However, there was no reports on ECL-aptasensors depended FB1 detection.

When incorporating with nanomaterials, the ECL-aptasensors exhibited enhanced performance for highly sensitive detection of targets.²¹⁻²⁴ In particular, Au NPs featured with excellent biological compatibility, the large specific surface and the superior conductivity, not only loaded many ECL labels on the surface, but also accelerated the electron transfer between ECL labels and electrode. And consequently the ECL efficiency and the sensitivity of biosensors could be substantially enhanced.²⁵⁻²⁷

A stable luminescent reagent with higher ECL efficiency was critical in the performance of ECL-aptasensors. In comparison to the most frequently utilized Ru complex, Ir cyclometalated complex showed better ECL efficiency, longer excited-state lifetimes and had been the subject of a growing interest. However, the lack of functional groups for biological labeling and the poor water-solubility of Ir cyclometalated complex restricted its applications in ECL-aptasensor.²⁸⁻³² Herein, carboxyl-functioned ionic [(ppy)₂Ir(dcbpy)]PF₆⁻ was synthesized and covered on the surface of Au NPs through mercaptoethylamine. In this study, the combination of Au NPs-[(ppy)₂Ir(dcbpy)]PF₆⁻ complex increased the ECL intensity and accelerated the electron transfer, and further enhanced the ECL performance of aptasensors. The ECL aptasensors were firstly applied for FB1 detection and the LOD was as low as to 0.27 ng/mL (Fig. 1). The Au NPs driven ECL-aptasensors provided a potentially simple and sensitive method for the quantification of mycotoxins in cereal.

Experimental

Materials

Sodium citrate, tetrachloroauric acid trihydrate (HAuCl₄·3H₂O) and 2-(Dibutylamino) ethanol (DBAE) were purchased from

Sigma-Aldrich. N-Hydroxysuccinimide (NHS), 1-ethyl-3-(3-dimethylaminopropyl) carbodiimide hydrochloride (EDC), mercaptoethylamine and lithium perchlorate (LiClO_4) were all purchased from Sinopharm chemical reagent Co., Ltd. All other chemicals were of analytical grade. The iridium complex $[(\text{ppy})_2\text{Ir}(\text{dcbpy})]\text{PF}_6^-$ were prepared in our laboratory.³² Aptamers of FB1 and partial complementary DNA (PC-DNA, Table S1) were synthesized by Sangon biotechnology Co., Ltd.

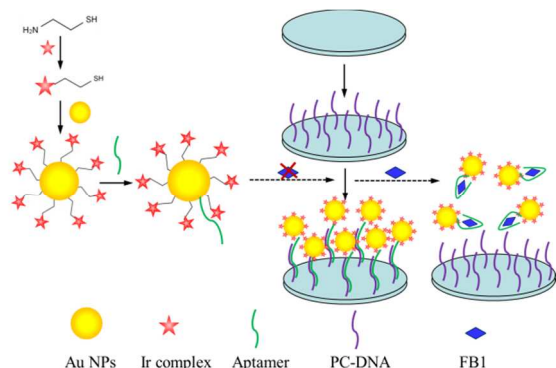


Fig. 1 Schematic illustration of Au NPs driven ECL aptasensors for FB1 detection.

Preparation of Au NPs-Ir complex

Au NPs were synthesized by sodium citrate reduction according to the previously reported methods.^{33, 34} An aliquot of 10 mL Au NPs was centrifuged at 5400 g for 10 min and re-suspended in ultrapure water with 1/20 original volume. The ionic iridium complex $[(\text{ppy})_2\text{Ir}(\text{dcbpy})]\text{PF}_6^-$ was firstly activated by EDC and NHS for 2 h, and then mercaptoethylamine was added into the above solution with the molar ratio of 1:1. The mixture further reacted for 8 h. Finally, mercaptoethylamine-Ir complex was modified on the surface of Au NPs through Au-S covalent bond, with the molar ratios of 50: 1, 100: 1, 200: 1, 500: 1 respectively. After 12 h, the mixtures were centrifuged at 5400 g for 10 min and re-suspended in 50% (by volume) methyl cyanide water solution.

Aptamers of FB1 were modified on the surface of Au NPs-Ir complex by Au-S covalent bond, with the molar ratios of 1:1. After 12 h, the conjugates were centrifuged to remove the unreacted aptamers, and the precipitate containing aptamers-Au NPs-Ir complex was re-suspended in 50% methyl cyanide solution.

Modification of Au Electrode

Au electrode was polished with 0.5 μm alumina slurry and washed by ethanol and ultrapure water for three times. An aliquot of 5 μL 10 μM PC-DNA was added onto the surface of Au electrode and allowed the reaction to proceed overnight. DNA modified Au electrode was rinsed thoroughly three times with ultrapure water to remove the unreacted PC-DNA, and dried by nitrogen gas.

Fabrication of ECL aptasensors

An aliquot of 10 μL aptamers-Au NPs-Ir complex was added onto the surface of PC-DNA modified Au electrode. The modified Au electrode was heated to 80 $^\circ\text{C}$ for 5 min and then slowly cooled to room temperature. Aptamers well hybridized with the PC-DNA at high temperature. Modified Au electrode was washed by ultrapure water for three times, and then was

immersed to seven different concentration of FB1 solution at 37 $^\circ\text{C}$ for 2 h. After rinsing, the functionalized electrode was used as the work electrode in the three-electrode system.

ECL determination of FB1 and the selectivity of sensors

Spiked experiments were carried out to evaluate the performance of the ECL aptasensor. An amount of 1.6, 8, 16 and 40 ng FB1 was respectively added into negative wheat flour with the final weight of 2 g. The mixture was dissolved into 2 mL 50% methanol water solution and was subsequently filtrated for three times to remove the precipitation, and FB1 molecules were dissolved in filtrate. The filtrate was collected solutions as the spiked solution and subjected for the ECL measurements.

The specificity of the ECL aptasensors was investigated at the presence of 100 ng/mL FB1, ochratoxin A (OTA), aflatoxin (AFT), L-cystein (L-cys), L-homocystein (L-Hcys) and their mixtures.

Instrumentation

ECL signals were carried out on the MPI-E ECL analyzer (Xi'an Remax Electro-Science & Technology Co. Ltd., China). A typical three electrode configuration was used in which Au electrode as the working electrode, a silver wire as the reference and a platinum wire as the counter electrode. UV-Vis spectra was measured using UV-visible spectrophotometer BioMate 3S (Thermo Fisher Scientific, USA). TEM images were obtained using a JEOL JEM-2100 microscope operating at an acceleration voltage of 200 kV. The luminescence imaging was obtained using ChemiScope 3000 fluorescence and chemical luminescence imaging system.

Results and discussion

Ir cyclometalated complexes were reported to be a novel ECL label and exhibited higher ECL intensity than that of the $\text{Ru}(\text{bpy})_3^{2+}$, but many of them showed poor water-solubility and was lack of active groups for biological labeling.^{32,35} Herein, ionic $[(\text{ppy})_2\text{Ir}(\text{dcbpy})]\text{PF}_6^-$ functioned with carboxyl groups was synthesized and could be well dissolved in 50% methyl cyanide solution (Fig. 2A-B).³⁵ The $[(\text{ppy})_2\text{Ir}(\text{dcbpy})]\text{PF}_6^-$ solution exhibited yellow in the visible light and showed reddish orange fluorescence in ultraviolet light (Fig. 2B). Compared to $\text{Ru}(\text{bpy})_3^{2+}$, $[(\text{ppy})_2\text{Ir}(\text{dcbpy})]\text{PF}_6^-$ exhibited strong ECL signal in LiClO_4 solution at the presence of 100 μM 2-(Dibutylamino)ethanol (DBAE) as a coreactant (Fig. 2C-D).

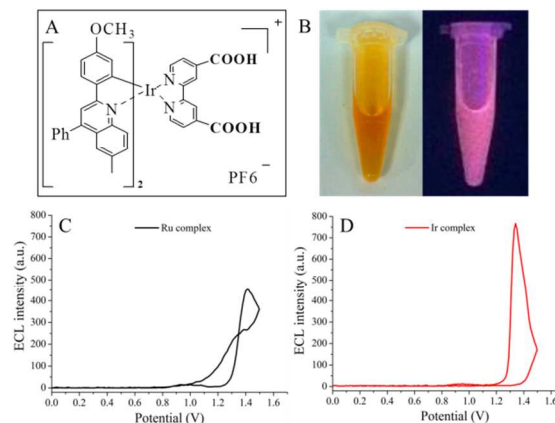


Fig. 2 (A) The structure of Ir complex ($[(ppy)_2Ir(dcbpy)]PF_6^-$). (B) The picture of Ir complex solution in visible light (left) and ultraviolet light (right). (C-D) ECL-potential curve of Ru complex and Ir complex.

As-prepared Au NPs showed uniform morphology (15 ± 2 nm) and good dispersivity as shown in Fig. 3A. The plasmon resonance peak of Au NPs was at 519 nm. Different amounts of Ir complex were capped on the surface of Au NPs by a linker of mercaptoethylamine. Because the citrated Au NPs would rapidly react with the amino-groups of mercaptoethylamine and induced the aggregation of Au NPs, ionic $[(ppy)_2Ir(dcbpy)]PF_6^-$ was firstly coupled with mercaptoethylamine through the formation of peptide bonds. The exposed sulfhydryl groups of mercaptoethylamine-Ir complex easily modified on the surface of Au NPs through Au-S bonds. As demonstrated in Fig. 3B, the plasmon resonance peak of Au NPs-Ir complex red-shifted from 519 nm to 525 nm, illustrating the successfully modification of Ir complex on the surface of Au NPs. There was also an enhanced absorption at 286 nm for Au NPs-Ir complex than signal Au NPs, ascribing to the spin-allowed ligand-centered $\pi-\pi^*$ transitions of the CN ligands for Ir complex. In addition, the intensity of absorption at 286 nm increased with the increase of the molar ratios between the Au NPs to Ir complex from 1 : 50 to 1 : 500.

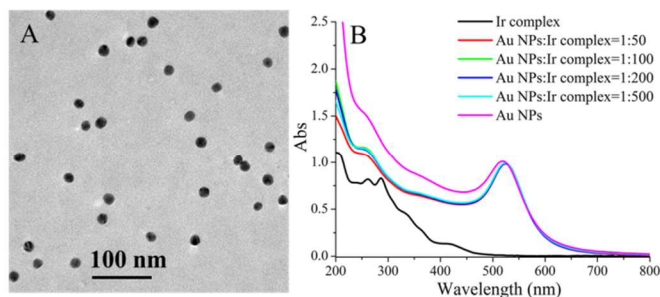


Fig. 3 (A) TEM images of Au NPs. (B) UV-vis spectra of Au NPs, Ir complex and the conjugates of Au NPs-Ir complex with different molar ratios.

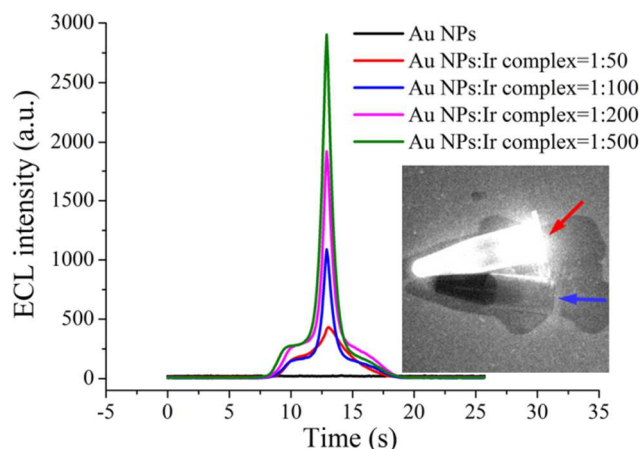


Fig. 4 ECL-time curves of Au NPs-Ir complex with different molar ratios. Insert, the luminescence imaging of Au NPs (blue arrow) and Au NPs-Ir complex (red arrow) with the molar ratio of 1:500.

The ECL performance of Au NPs-Ir complex was a critical factor for the biosensor application. The strong ECL intensity of Au NPs-Ir complex determined the high sensitivity and good accuracy of ECL-aptasensors. As illustrated in Fig. 4, with the increasing molar ratios from 1 : 50 to 1 : 500 for Au

NPs-Ir complex, the ECL signal of the conjugates of Au NPs-Ir complex was correspondingly increased from 431 to 2902 which was measured in $LiClO_4$ solution in the presence of 1 mM DBAE as a coreactant. These results were accorded to our previous assumptions. Furthermore, Au NPs-Ir complex exhibited obvious bright luminescence imaging under the exciting light of 395 nm,^{36, 37} while there was no luminescence for single Au NPs. The enhanced ECL signal of Au NPs-Ir complex mainly ascribed to the excellent ECL intensity of ionic $[(ppy)_2Ir(dcbpy)]PF_6^-$, the large surface-to-volume property and the superior conductivity of Au NPs. Au NPs not only adsorbed more ionic $[(ppy)_2Ir(dcbpy)]PF_6^-$ on the surface and amplified the ECL intensity, but accelerated the electron transfer between $[(ppy)_2Ir(dcbpy)]PF_6^-$ and electrode, hence increasing the ECL efficiency. In conclusion, Au NPs-Ir complex with the molar ratio of 1 : 500 exhibited the strongest ECL intensity and could be served as an alternative ECL nanoprobe for the detection of FB1.

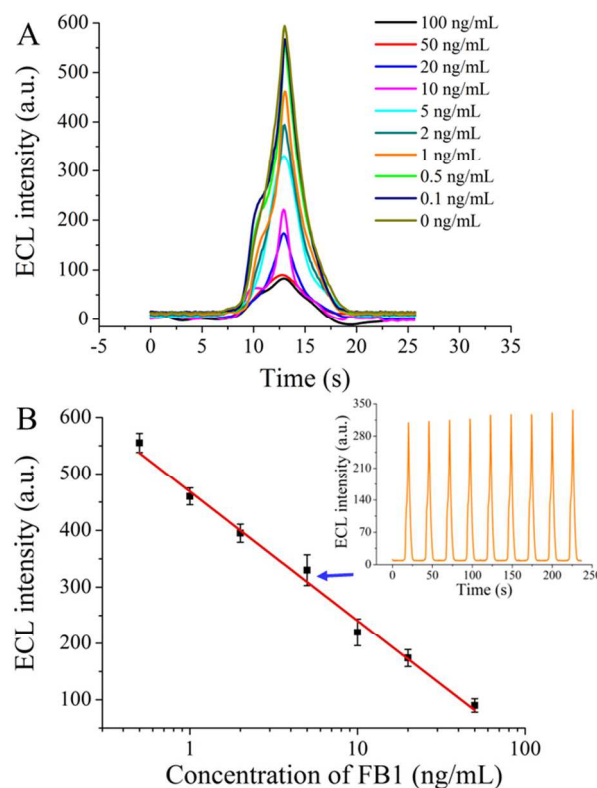


Fig. 5 (A) ECL profiles of the proposed ECL aptasensors in different concentration of FB1 solution. (B) The standard curve of the determination of target FB1. Insert in B, at 5 ng/mL FB1, the ECL stability of Au NPs-Ir complex after nine continuous CV cycles.

PC-DNA and FB1 competitively combined to aptamers modified Au NPs-Ir complex (Fig. S1). With the increasing concentration of FB1, more aptamers on Au NPs-Ir complex were specifically combined to FB1. After rinsing, the captured amount of Au NPs-Ir complex by PC-DNA modified electrode would be reduced, resulting in low ECL signals. The ECL intensity of aptasensors was inversely proportional to the FB1 concentration. As shown in Figure 5A, with the decrease of FB1 concentration from 100 ng/mL to 0.1 ng/mL, the ECL signal of aptasensor was correspondingly increased. But for 100 ng/mL and 50 ng/mL FB1, there were no obvious changes in the ECL intensities, presumably because the limited aptamers

could not recognize the excess amount of FB1. Similarly, in the low concentration range, i.e., for 0.5 ng/mL, 0.1 ng/mL and 0 ng/mL FB1, the changes in the ECL intensity were also small, **Table 2**. Comparison of FB1 detection based on different analytical methods.

due to the limitation of aptasensor sensitivity. In the range of 0.5 to 50 ng/mL, a standard curve between the

Methods	Characteristics	LODs (ng/mL)	Refs
Fluorescence Resonance Energy Transfer	Depended on the unstable fluorescence donors and acceptors; The non-specific adsorption, strong background emission from the biology matrix and the long aptamers of FB1 counted against the accuracy.	0.01-0.1	7, 8
Fluorescence based Immunochromatographic Assay	Required FB1 monoclonal antibody and the purchased fluorescence microspheres. The large size of microspheres affected their flowability in the strips. Limited by poor quantitative discrimination.	0.12	9
ECL-aptasensor	The combination of high ECL efficiency and high affinity and specificity of aptamers. Au NPs driven ECL aptasensor had weak background noise and was firstly applied in the detection of FB1.	0.27	This work
Indirect competitive ELISA	Required complicated and multi-step operations, False positive results and low sensitivity limited its application.	1.0-5.4	4, 5
High Performance Liquid Chromatography	Required expensive instruments and liquid-liquid extraction and preliminary clean-up steps.	10	6

FB1 concentrations and ECL intensities of Au NPs-Ir complex was established, which showed a good correlation of $R^2 = 0.992$. Besides, the ECL aptasensors showed stable ECL response after nine continuous CV scanning, implying a good repeatability of the analytic methods (Fig. 5B, insert). The LOD was estimated to be 0.27 ng/mL based on the three time standard deviations of the baseline noises.

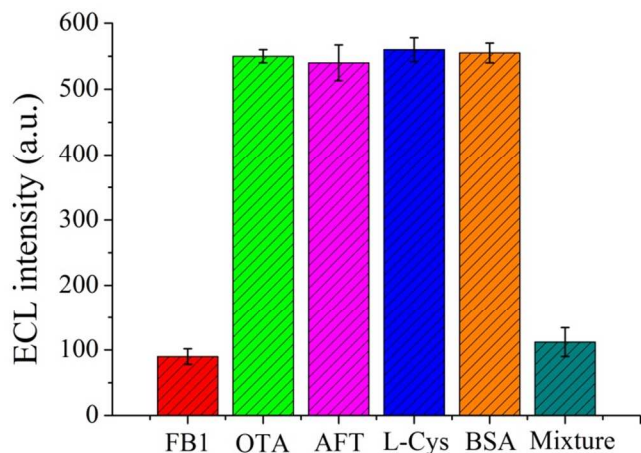


Fig. 6 ECL response of the aptasensor for 100 ng/mL FB1, OTA, AFT, L-cys, L-Hcys and their mixtures.

Table 1. The recovery of FB1 from the negative wheat flour.

Name	Spiked concentration (ng/mL)	Detected concentration Mean ^a ±SD ^b (ng/mL)	Recovery (%)
1	0.8	0.86 ± 0.05	107.5
2	4.0	4.13 ± 0.3	103.3
3	8.0	7.81 ± 0.6	97.6
4	20	19.72 ± 0.8	98.6

^aThe mean of three experiments. ^bSD = standard deviation.

In order to evaluate the feasibility of the proposed ECL aptasensors, specificity tests and spiked experiments were both conducted. As demonstrated in Fig. 6, the ECL aptasensor exhibited strong ECL intensity in the presence of OTA, AFT, L-cys and L-Hcys, but showed low ECL signal for FB1 and the mixtures of FB1, OTA, AFT, L-cys and L-Hcys, attributing the specific affinity between aptamers and FB1.^{7-8, 15} The good selectivity was sufficient for the application of the ECL aptasensors in the detection of FB1. Investigation of matrix effect was an important part for the practical applications of the ECL aptasensor. Thus spiked experiments were performed by adding FB1 into the negative wheat flour (Table 1). The results showed the recoveries were in the range of 97.6% to 107.5%, which validate the practical value of the ECL-aptasensor. In comparison to the traditional ELISA and the reported fluorescence methods (Table 2), Au NPs driven ECL aptasensor exhibited higher sensitivity, better accuracy, excellent repeatability and simple operations, and can be served as an effective tool for mycotoxin detection.

Conclusions

In this work, a simple, accurate, selective Au NPs driven ECL-aptasensor was first developed for the sensitive detection of FB1. In comparison to Ru complex, the stronger ECL intensity and longer excited-state lifetimes enabled Ir cyclometalated complex to be an alternative ECL reagent. The superior specific surface area and the excellent conductivity of Au NPs increased the amount of Ir cyclometalated complex on the surface and accelerated the electron transfer, which further amplified the ECL intensity and enhanced the ECL efficiency. The LOD was down to 0.27 ng/mL. The sensitivity may be future enhanced by synthesizing Ir cyclometalated complex with higher ECL efficiency. The proposed Au NPs-Ir complex driven ECL-aptasensors showed a potential prospect in the sensitive mycotoxin detection.

Acknowledgements

This work is financially supported by the National Natural Science Foundation of China (21175060, 21403090), the Fundamental Research Funds for the Central Universities (No. JUSRP11424) and the 111 Project (B13025).

Notes and references

The Key Lab of Food Colloids and Biotechnology, Ministry of Education, School of Chemical and Material Engineering, Jiangnan University, Wuxi, Jiangsu, 214122, PRC. E-mail: qsong@jiangnan.edu.cn;

† Electronic Supplementary Information (ESI) available: The sequences of aptamer and the partial complementary DNA (Table S1), The detail schematic illustration of Au NPs-Ir complex driven ECL-aptasensors (Fig. S1). See DOI: 10.1039/b000000x/.

- 1 Y. Quan, Y. Zhang, S. Wang, N. Lee and I. R. Kennedy, *Anal Chim Acta*, 2006, **580**, 1-8.
- 2 Y. J. Sheng, W. X. Jiang, S. De Saeger, J. Z. Shen, S. X. Zhang and Z. H. Wang, *Toxicon*, 2012, **60**, 1245-1250.
- 3 S. M. Ling, J. Pang, J. J. Yu, R. Z. Wang, L. C. Liu, Y. L. Ma, Y. M. Zhang, N. Jin and S. H. Wang, *Toxicon*, 2014, **80**, 64-72.
- 4 S. Ling, J. Pang, J. Yu, R. Wang, L. Liu, Y. Ma, Y. Zhang, N. Jin and S. Wang, *Toxicon*, 2014, **80**, 64-72.
- 5 Y. Sheng, W. Jiang, S. De Saeger, J. Shen, S. Zhang and Z. Wang, *Toxicon*, 2012, **60**, 1245-1250.
- 6 W. S. Khayoon, B. Saad, B. Salleh, N. A. Ismail, N. H. Abdul Manaf and A. Abdul Latiff, *Anal Chim Acta*, 2010, **679**, 91-97.
- 7 S. J. Wu, N. Duan, X. L. Li, G. L. Tan, X. Y. Ma, Y. Xia, Z. P. Wang and H. X. Wang, *Talanta*, 2013, **116**, 611-618.
- 8 S. Wu, N. Duan, X. Ma, Y. Xia, H. Wang, Z. Wang and Q. Zhang, *Anal Chem*, 2012, **84**, 6263-6270.
- 9 Z. H. Wang, H. Li, C. L. Li, Q. Yu, J. Z. Shen and S. De Saeger, *J. Agr. Food. Chem.*, 2014, **62**, 6294-6298.
- 10 S. Wang, Y. Quan, N. Lee and I. R. Kennedy, *J. Agr. Food. Chem.*, 2006, **54**, 2491-2495.
- 11 L. Shen, Y. Sun, J. Li, L. Chen, L. Li, G. Zou, X. Zhang and W. Jin, *Talanta*, 2012, **89**, 427-432.
- 12 M. Yang, B. Jiang, J. Xie, Y. Xiang, R. Yuan and Y. Chai, *Talanta*, 2014, **125**, 45-50.
- 13 X. Y. Wang, A. Gao, C. C. Lu, X. W. He and X. B. Yin, *Biosens Bioelectron*, 2013, **48**, 120-125.
- 14 W. Cheng, S. Ding, Q. Li, T. Yu, Y. Yin, H. Ju and G. Ren, *Biosens Bioelectron*, 2012, **36**, 12-17.
- 15 M. McKeague, C. R. Bradley, A. De Girolamo, A. Visconti, J. D. Miller and M. C. DeRosa, *Int. J. Mol. Sci.*, 2010, **11**, 4864-4881.
- 16 J. Zhao, Y. Zhang, H. Li, Y. Wen, X. Fan, F. Lin, L. Tan and S. Yao, *Biosens Bioelectron*, 2011, **26**, 2297-2303.
- 17 M. Yang, B. Jiang, J. Xie, Y. Xiang, R. Yuan and Y. Chai, *Talanta*, 2014, **125**, 45-50.
- 18 M. McKeague, C. R. Bradley, A. D. Girolamo, A. Visconti, J. D. Miller and M. C. DeRosa, *Int. J. Mol. Sci.*, 2010, **11**, 4864-4881.
- 19 H. Huang and J. J. Zhu, *Biosens Bioelectron*, 2009, **25**, 927-930.
- 20 G. Jie and J. Yuan, *Anal Chem*, 2012, **84**, 2811-2817.
- 21 C. Fu, Q. Xu, X. Wei and J. Li, *RSC Advances*, 2014, **4**, 26102-26107.
- 22 M. Hesari, M. S. Workentin and Z. Ding, *RSC Advances*, 2014, **4**, 29559-29562.
- 23 J. Lei and H. Ju, *Chem Soc Rev*, 2012, **41**, 2122-2134.
- 24 S. Deng, J. Lei, Y. Huang, X. Yao, L. Ding and H. Ju, *Chem Commun (Camb)*, 2012, **48**, 9159-9161.
- 25 M. Freitas, S. Viswanathan, H. P. Nouws, M. B. Oliveira and C. Delerue-Matos, *Biosens Bioelectron*, 2014, **51**, 195-200.
- 26 B. Kavosi, R. Hallaj, H. Teymourian and A. Salimi, *Biosens Bioelectron*, 2014, **59**, 389-396.
- 27 H. Kuang, W. Chen, D. Xu, L. Xu, Y. Zhu, L. Liu, H. Chu, C. Peng, C. Xu and S. Zhu, *Biosens Bioelectron*, 2010, **26**, 710-716.
- 28 K. N. Swanick, S. Ladouceur, E. Zysman-Colman and Z. Ding, *RSC Advances*, 2013, **3**, 19961-19964.
- 29 Y. Dong, Z. Ni, J. Zhang, B. Tong and X. Chu, *Journal of Luminescence*, 2013, **136**, 165-171.
- 30 Y. P. Dong, M. J. Shi, B. H. Tong and Q. F. Zhang, *Luminescence*, 2012, **27**, 414-418.
- 31 M.-J. Li, Y.-Q. Shi, T.-Y. Lan, H.-H. Yang and G.-N. Chen, *J. Electroanal. Chem*, 2013, **702**, 25-30.
- 32 X. Ni, T. Li and Q. Song, *J. Electroanal. Chem*, 2014, **719**, 30-34.
- 33 Y. Zhao, L. Xu, W. Ma, L. Liu, L. Wang, H. Kuang and C. Xu, *Small*, 2014, DOI:10.1002/sml.201401203.
- 34 Y. Zhao, L. Xu, W. Ma, L. Wang, H. Kuang, C. Xu and N. A. Kotov, *Nano Lett*, 2014, **14**, 3908-3913.
- 35 T. Li, M. Cui, G. Ran and Q. Song, *Dyes and Pigments*, 2015, **112**, 1-7.
- 36 C. Zong, J. Wu, C. Wang, H. Ju and F. Yan, *Anal Chem*, 2012, **84**, 2410-2415.
- 37 C. Zong, J. Wu, J. Xu, H. Ju and F. Yan, *Biosens Bioelectron*, 2013, **43**, 372-378.